Journal of Thermal Analysis and Calorimetry (2023) 148:11955–11968
https://doi.org/10.1007/s10973-023-12472-y

Investigating the modified thermoelectric generator system performance

Abd El-Moneim A. Harb[1] · Khairy Elsayed[1] · A. E. Kabeel[2,5] · Mahmoud Ahmed[3,4] · Ahmed Abdo[2]

Received: 25 January 2023 / Accepted: 9 August 2023 / Published online: 12 September 2023

Abstract

It is essential to enhance the performance of the thermoelectric generator as lower efficiencies are obtained recently. This could be achieved by changing its dimensions in addition to copper strip thickness. The present study is performed to obtain the best dimensions of the *P–N* legs considering the interaction between all variables. To do this, a comprehensive TEG model is achieved in addition to utilizing the single-objective optimization technique. The main performance metrics, including electricity production and conversion efficiency, are assessed, and contrasted with the conventional TEG system since the simulation. The length of the legs and their cross-sectional area were shown to significantly affect power production. The thickness of the conducting plate, in contrast, barely matters. For instance, a *P–N* pair with legs that have a 2 mm^2 cross-sectional area generates 0.4 W and 1.3 W for temperature differences of 480 °C and 980 °C, respectively. Furthermore, the equivalent efficiencies are 4.41% and 6.73%, respectively. Using the genetic algorithm revealed that the ideal values for the leg cross section, leg length, and conducting plate thickness are 1.84 mm^2, 0.5 mm, and 0.44 mm, respectively. Once compared to the conventional system, using the optimization method results in an improvement in power production and conversion efficiency of about 247% at a temperature differential of 980 °C.

Keywords Thermoelectric generator · Single-objective optimization · Genetic algorithm · Semiconductors · Conversion efficiency

List of symbols

A	Cross-sectional area of leg (mm^2)
A_n	Leg cross-sectional area (*N*-type)
A_p	Leg cross-sectional area (*P*-type)
dx	Thermoelectric element length (mm)
E_{max}	Maximum efficiency
H	Height of Leg (mm)
I	Electrical flow (A)
K	Thermal conductivity (W m^{-1} K^{-1})
K_n	Thermal conductivity of (*P*-type) Leg
K_P	Thermal conductivity of (*N*-type) Leg
L	Length of leg (mm)
L_t	Thickness of electrical conducting plate (mm)
P_{max}	Maximum power output (W)
$P_{max\text{-}t}$	Theoretical maximum power output (W)
P_o	Power output generation (W)
R	Internal resistance of the semiconductors (Ω)
R_L	Load resistance (Ω)
T_c	The temperature of cold side (°C or K)
T_m	Melting point (°C or K)
T_h	The temperature of the hot side (°C or K)
ΔT	Temperature difference (°C or K)
W_n	Width of (*N*-type) Leg (mm)
W_p	Width of (*N*-type) Leg (mm)
ZT	Figure of merit

✉ Abd El-Moneim A. Harb
moneimharb@m-eng.helwan.edu.eg

✉ A. E. Kabeel
kabeel6@f-eng.tanta.edu.eg

[1] Department of Mechanical Power Engineering, Faculty of Engineering at El-Mattaria, Helwan University, Helwan, Egypt

[2] Mechanical Power Engineering Department, Faculty of Engineering, Tanta University, Tanta, Egypt

[3] Energy Resources Engineering Department, Egypt- Japan University of Science and Technology (E-JUST), Alexandria, Egypt

[4] Mechanical Engineering Department, Assiut University, Assiut 71516, Egypt

[5] Faculty of Engineering, Delta University for Science and Technology, Gamasa, Department of Mechanical Engineering, Islamic University of Madinah, Medina 42351, Saudi Arabia, Egypt

Greek symbols

α	Seebeck coefficient (μV K^{-1})
η_{max}	Maximum thermal conversion efficiency
ρ_p	Qualitative resistance of (*P*-type) (Ω m)
ρ_n	Qualitative resistance of (*N*-type) (Ω m)
σ	Electrical conductivity (Ω^{-1} m^{-1})

Subscript

c	Cold
h	Hot
L	Load
p	Plate

Abbreviations

DoE	Design of experiment
LHS	Latin hypercube sampling
PV	Photovoltaic
RBFNN	Radial basis function neural network
STEG	Solar thermoelectric generator
TE	Thermoelectric
TED	Thermoelectric device
TEG	Thermoelectric generator

Introduction

Increasing energy demand and environmental pollution caused by traditional thermal sources such as internal combustion engines and power plants become serious issues. Thus, scientists have been working on the new promoted power devices such thermoelectric generator (TEG) that can convert heat directly into electricity [1]. Its operation is based on thermoelectric effects such as Seebeck, Peltier, and Thomson. [2]. Vast engineering applications are capable of employee TEG as recovery device, for example, recovering waste heat in automobile, steel industries, cook stoves, and power plants, as well as body skin [3–7]. Even it has taken long time to be commercially widespread due to its low conversion efficiency which is less than 5% [8]. Multiple strategies to improve the TEG system's performance were examined by certain researchers. These studies are categorized into three main types. First category considers the increasing of TEG figure of merit (ZT) based on the materials construction improvement. Kanimba and Tian [9] have presented a new dimensionless figure of merit. Many scientists are working hard to create a new alloy with a better ZT and power factor [10–14]. Second category considers TEG installation method inside an engineering system such as TEG recovering waste heat from power station condenser or exhausted gases from heat engines. Consequently, the overall efficiency of the system improves [15–17]. Third category introduces a best TEG module to help designer to produce TEG devices with the highest conversion efficiency [18].

Multiple studies examined how well TEG modules functioned, and Chen et al. [19] gave an analytical solution for the TEG governing equation. In addition, thermoelectric properties of a TEG module are assumed as a constant. A new expression for temperature distribution, output power and conversion efficiency was introduced. Meng et al. [4] used Taylor expansion to ease the power correlation. Specified temperature difference mostly along the *P–N* legs, both the warm and cold sides of the system, is supposed in their study. Further to that, the optimal parameters for leg length and electrical charge were determined. Ma et al. [20] studied the effect of the TEG geometry such as the semiconductors leg cross-sectional area and length in addition to the electrical conducting plate thickness on the system performance. The length was ranged from 0.5 mm to 4 mm, and the leg cross-sectional area was ranged from 0.2 mm^2 to 2 mm^2. In addition, the thickness of the conducting plate was ranged from 0.1 mm to 1 mm. Their findings concluded that at a constant leg length, power is enhanced by leg cross-sectional area increase. Moreover, at 1.00 mm^2 leg cross-sectional area, the output power decreases with increasing leg length. The earlier effects are due to the reduction in internal resistance. This is due to the decrease in leg length or the increase in cross-sectional area. For conducting plate thickness effect, both the power and the efficiency change with varying the plate thickness. The optimal power and efficiency are in the range between of 0.125 mm and 0.5 mm. The increasing in the conducting plate thickness leads to increase the heat loss and reducing the power output and conversion efficiency accordingly. Shen et al. [21] studied the effect of the leg length at different heat transfer coefficient where it was ranged from 1 to 10 mm. Findings showed that as the leg length increases the power output decreases. At low heat transfer coefficient equals zero and varying the leg length from 1 to 10 mm, the maximum power of 0.35 W was obtained at the value of 1 mm and the corresponding conversion efficiency was around 3.4%. Oh et al. [22] studied the effect of the leg length of the thermoelectric generator performance at different temperature difference between the cold and the hot side. It was seen that the temperature difference significantly affects the output power as temperature difference increase leads to output power enhancement. However, the opposite effect is achieved by leg length where its increase caused a reduction in the output power. The predicted optimal length was about 2.6 mm for all temperature difference and was independent of the temperature difference. Ali et al. [23] utilized an exponential parametric function to calculate the variations in cross-sectional area of a single *P–N* pair and found an optimal value that maximizes power and conversion efficiency. Yamashita [24] investigated the effect of semiconductor temperature-dependent properties on current, maximum power, and efficiency, considering linearity and nonlinearity in the properties of

the *P–N* couple. Wang et al. [25] introduced an analytical method in addition to a new algorithm to figure out the main parameters of a thermoelectric module. Ali and Yilbas [26] present a new material with linear property variation along its length. In their study, they showed that the proposed one has greater outcome electricity and conversion efficiency than conventional materials. Kalteh and Akhlaghi [27] studied the effect of Thomson effect on a TEG performance. In addition, the effect of Thomson heat on the best values for two different alloys is evaluated. Zhang et al. [28] studied the performance of two-stage TEG model depending on hypercube sampling. A TEG system with a radiation heat sink was proposed by Liu et al. [29]. They concluded that the proposed system has an enormous potential to be used in electronic applications.

Arora et al. [30] contrasted and perfected the productivity of both a single- and multi-stage TEG. A theoretical solution is used to analyze the system. Marvao et al. [31] reported a comprehensive optimization for a TEG as a heat recover unit utilized in an automobile exhaust. In their study, the output power is examined as the objective function. Optimization for constant temperature thermoelectric generator with constant temperature boundary condition has been done by Xu et al. [32]. In their study, the goal function was power output. Sun et al. [33] worked to optimize a two-stage TEG device design. They considered the power output and entropy generation as the objective function. Nozariasbmarz et al. [34] conducted research and optimization of TEGs for wearable body heat collection.

Following a recent literature study, small number of studies were conducted using the optimization approach to figure out the proper dimensions for the *P–N* module. Furthermore, the interaction between the TEG variables such as the leg area, conducting plate thickness and the leg length is not considered. Number of factors need to be looked at to reach the best design point for the TEG system. Thus, the originality of the present study is based on using a single-objective optimization to study the effect of all variables such as the leg area, conducting plate thickness in addition to the leg length. Therefore, a comprehensive three-dimensional model of the TEG system, as well as an optimization genetic scheme, is constructed. The simulation is used to examine and compare the major performance measures, such as power output and conversion efficiency, with the classic TEG system.

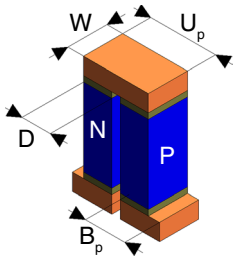

Fig. 2 The detailed schematic diagram of thermoelectric couple

Physical model

Figure 1 shows schematic of the TEG system considered in the present study. The main components of this system are ceramic layers, copper strips and *P–N* legs. Thermoelectric unit is a major part of a TEG system. This device has both hot and cold sources, as well as multiple thermocouple units in the center that are all linked. The three essential components of each thermoelectric device are electrical conducting plates (such as copper), n/p type semiconductors, and solder layers to connect the *P–N* legs to the conducting slices, as shown in Fig. 1.

Figure 2 shows a schematic diagram and main dimensions of a single *P–N* couple as specific unit of TEG system. Based on the configuration, A, t_p, and L indicate cross-sectional

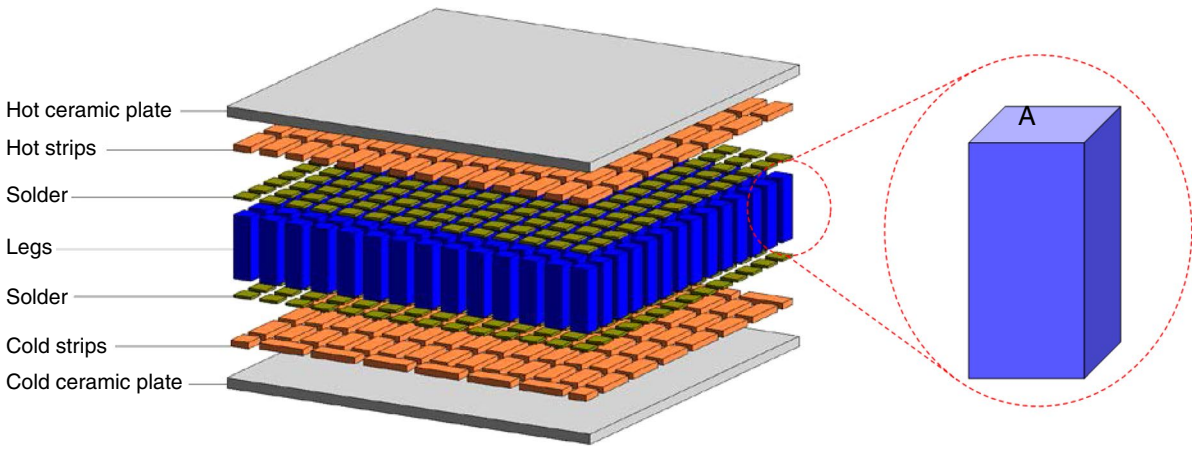

Fig. 1 Three-dimensional views of the thermoelectric system

Table 1 The chosen range of design variables

Variable	A/mm^2	t_p/mm	L/mm
Minimum	0.2	0.1	0.5
Maximum	2.0	1	4

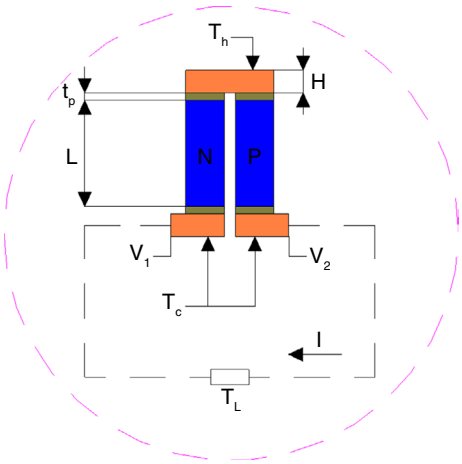

Fig. 3 The operation of a *P–N* junction. The dotted lines in the circuit are used to show loop current generation, which was absent in the simulation

area of leg, strips thickness, and leg length, in that order. Before starting TEG numerical simulation, an optimization process was performed by MATLAB software to figure out the suitable range for TEG dimensions A, t_p, and L to reduce number of iterations implemented simulation software to safe time needed to reach the better design achieving good output electricity and conversion efficiency. The detailed results of MATLAB modules will be introduced in Section "Optimization procedures". It should be noted that the performance of the TEG system is overly sensitive to the values of the decision variables A, tp, and L. Table 1 is a list of the decision variable ranges. These numbers are set up based on the TEG system's actual operational circumstances.

As shown in Fig. 3, the *P–N* junction made from silicon germanium (SiGe) where *P–N* legs are equal in length. Similarly, the cross-sectional areas are equal. When the ends of the thermoelectric unit are subjected to cold and hot sources, an electric potential will be created (V_1–V_2) that generates a loop current I. The energy conversion is caused due to Seebeck effect that explains that heat transferring through thermoelectric *N–P* legs and under a temperature difference will be converted directly into electricity between the TEG edges [2]. The cold and hot side temperature are showed by T_c and T_h, respectively. Table 2 provides a summary of the physical features of many TEG materials, including silicon germanium (SiGe).

The study of the thermoelectric generator is performed through two main steps. In the first step, the effect of each decision variable listed in Table 1 on the performance parameters, out power and conversion efficiency is examined by using MATLAB software. In the second step, a numerical solution using ANSYS software is performed to analyze the TEG system and calculate the power output as an objective function. Consequently, the conversion efficiency can be calculated. Only one pair of *P–N* couple made from SiGe alloy is examined in this work. Finally, the predicted results are compared with the numerical result provided by [20] as will be introduced in the result Section "Results and discussion".

Theoretical analysis

The theoretical analysis of the *P–N* junction can be implemented through the study of the governing equations of the TEG system. Use a single-objective optimization technique to reach the greatest performance of the TEG system. Consequently, available information from the optimization process can be invested to build a numerical flexible model ANSYS software which help designer to create an effectively high-performance thermoelectric module to generate electricity from available thermal sources including conventional and renewable resources [35].

Governing equations

A three-dimensional thermal-electric model is developed to analyze the system. The dimensions, materials and shapes of the TEG directly affect the performance parameters. Equation (1, 2) is used to calculate the convention efficiency η [20]. Regarding the largest TEG efficiency, the formula of maximum conversion efficiency can be stated (2) as following.

Table 2 The properties of the thermoelectric unit used in the current study

Material	Melting point/°C	Seebeck coefficient/μV K^{-1}	Thermal conductivity/W m^{-1} K^{-1}	Electrical conductivity/Ω m	Figure of merit/K^{-1}
SiGe	1177	115 (P)(N)	5.56	1.00×10–5	2.38×10–4
CU	1083	–	394.50	1.84×10–8	–
63Sn-37Pb	183	–	50.00	1.45×10–7	–

Regarding the maximum output power condition, the formula of maximum output power can be written as seen in Eq. (3).

$$\eta = \frac{\Delta T \cdot R_{\mathrm{L}}}{T_{\mathrm{h}}\left(R + R_{\mathrm{L}}\right) - \frac{\Delta T \cdot R}{2} + \frac{\left(R+R_{\mathrm{L}}\right)^2}{ZR}} \tag{1}$$

where: ΔT, T_h T_c, R and R_L are temperature difference, hot side temperature, cold side temperature, internal resistance, and external load resistance, respectively [19].

$$\eta_{\max} = \Delta T \cdot \frac{\sqrt{1+Z\overline{T}} - 1}{T_{\mathrm{h}}\sqrt{1+Z\overline{T}} + T_{\mathrm{c}}} \tag{2}$$

$$P_{\max} = \alpha^2 (T_{\mathrm{h}} - T_{\mathrm{c}})^2/(4R) \tag{3}$$

Computational study supplies a versatile and economical method for finding optimum parameters of TEG devices. The analysis of thermoelectric devices needs the simultaneous computation of thermoelectric effects and heat transfers. [14]. The governing equations of heat transfer in steady state conditions and electrical current can be written in vector form as follows [35]:

$$\overrightarrow{\nabla}.\vec{J} = 0 \tag{4}$$

$$-\vec{\nabla} \cdot \vec{q} + Q^{\cdot} = 0 \tag{5}$$

Heat is reversible transfer by Peltier effect and by Fourier's law as the following:

$$\vec{\mathrm{q}} = \alpha \mathrm{T}\vec{J} - \kappa\overrightarrow{\nabla}T \tag{6}$$

The electrical field density at any location is decided by the combination of Seebeck and Ohm effects as follows:

$$\vec{E}_f = \alpha\Delta\overrightarrow{\mathrm{T}} + \rho\vec{J} \tag{7}$$

$$\mathrm{Q}^{\bullet} = \vec{E}_{\mathrm{f}}.\vec{J} \tag{8}$$

By substituting Eqs. (6, 7, and 8) into Eq. (5), the temperature distribution in the interior of thermoelectric generator (TEG) is given by:

$$\overrightarrow{\nabla}.\left(\kappa\overrightarrow{\nabla}T\right) + \rho\vec{J}.\vec{J} - T\frac{\mathrm{d}\alpha}{\mathrm{d}T}\overrightarrow{\nabla}T.\vec{J} = 0 \tag{9}$$

where: $T\frac{\mathrm{d}\alpha}{\mathrm{d}T}$ is defined as Thomson coefficient, and $\kappa, \alpha, J,$ and ρ are solid thermal conductivity, Seebeck coefficient, current density, and electrical resistivity, respectively.

Numerical procedures

Currently, in this study ANSYS FLUENT 19-R2 was used to solve the TEG models. The finite volume approach was used to resolve the governing equations with boundary conditions. The geometry supplied is used to run three-dimensional simulations in Fig. 3. The length of each part is mentioned, and all parts have the same width. In addition, the hot and cold sides of the thermoelectric unit are subjected to constant temperature T_h and T_c, respectively. The external sides of the computational domain are assumed to be adiabatic. To achieve maximum power and conversion efficiency for thermoelectric unit, the terminal sides of the unit are subjected to voltage load as shown in Fig. 3. As wrote down in this figure, the two parameters V_1 and V_2 represent the voltage at the N and P ends, respectively. The value of V_1 is 0 V, while V_2 is found from the simulation which is higher than 0 V by a certain value.

Mesh independent test

A grid independent test was conducted to get an independent value for the heat flow by varying the number of grids. According to the mesh test shown in Fig. 4, the heat flux value is unaffected by a cell count increase of more than 27,200. The present numerical simulation uses this cell number as a result.

Optimization procedures

Figure 5 shows the main steps of the proposed optimization cycle followed by more detailed descriptions. In the present study, ANSYS-Thermoelectric code is utilized to supply the TEG couple geometry to perform the required

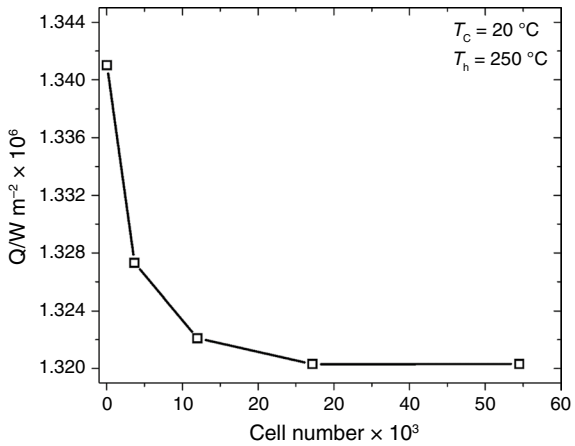

Fig. 4 Mesh independent test for computational domain of thermoelectric couple

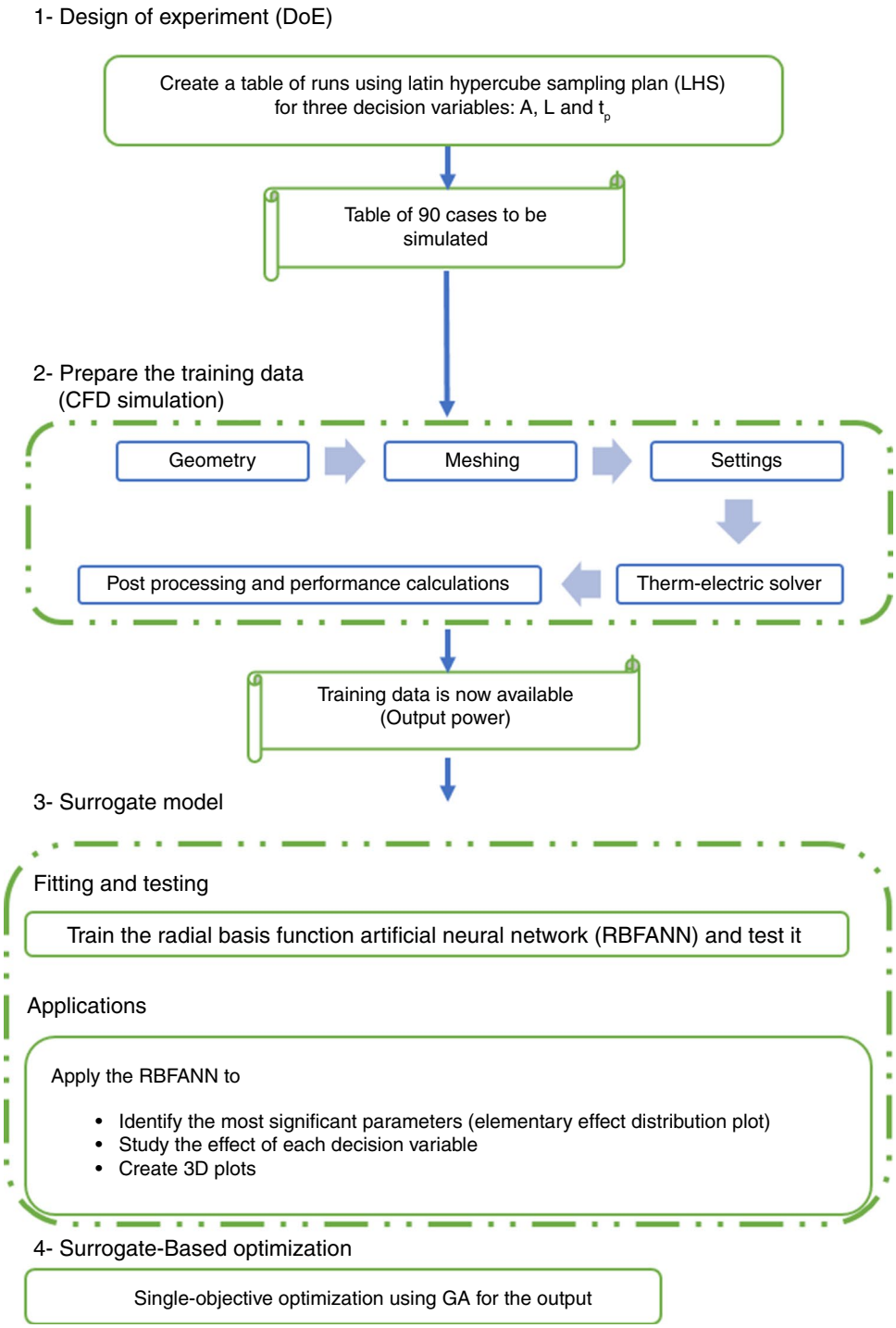

Fig. 5 Flowchart for surrogate-based optimization technique

simulations. In addition, MATLAB code was used for performing the single-objective genetic optimization [36]. To optimize the design variables, an optimization algorithm was chosen and used. So, a genetic algorithm (GA) was used for single-objective optimization technique that is used to reach the best performance of the TEG system. The cross-sectional area of leg, the strips thickness and the leg length are considered as a design variable, while the temperature of the cold side is kept constant at 20 °C. After the separate study of each decision variable on the TEG performance, an optimization technique is performed to investigate the effect of interactions between all variables and to supply optimum output power and consequently, the conversion efficiency can be estimated. The best values of the design variables in addition the output power obtained from the optimization algorithm are listed in Table 3. As shown in this table, there

Table 3 The results of the single-objective function

A/ mm^2	t_p/mm	L/mm	Optimization algorithm/W	CFD/W	Error/%
1.94354	0.284309	0.500168	2.56	2.39	6.5

are a good agreement between the output power obtained from the optimization algorithm with the corresponding value from CFD analysis with relative error around 6.5%.

Results and discussion

This section is including three subsections. First, the model validation is presented. The second subsection discusses the separate effect of each design variable on the performance parameters of the thermoelectric system. Lastly, comparison between the performance parameter of the modified and conventional thermoelectric unit is presented.

Model validation

The current investigated model was confirmed with the available theoretical and experimental results. It is confirmed by experimental work done by Yang et.al. [37] as they evaluate experimentally the performance of a TEG module make from Bismuth–telluride material and working under different values of hot–cold sides temperature. Additionally, the accessible numerical results obtained by [20] were compared to the current numerical findings to validate the existing model. Two sets of data were used for the validation. In the first set, a comparison of the thermoelectric unit's estimated maximum power output and maximum efficiency was made while considering the solder layers and the numerical results of [20]. For the second set, numerical findings from [20] were compared with the results of the thermoelectric unit's estimated power output without solder layers.

Figure 6 presents model validation with an experimental TEG module study by Yang et al. [37]. The heat source for the used TEG is a copper block that has four tubular heaters implanted in it. Each thermoelectric module is made up of 241 pairs of p- and n-type TE legs that are placed between the hot-side and cold-side substrates of a ceramic insulator and connected in series. TEG is made of (Bi_2Te_3, TEP1-24,156–2.4) with a dimension of 56 mm × 56 mm × 4 mm. The comparison is based on the values of generated voltage and output power which are shown in Fig. 6. The maximum error is about 7% in voltage difference and about 8% in the generated output power. The main reason of this error is the assumption in the numerical study that neglect the effects of connection between the five TEG modules and the solders material between the layers of TEG.

Comparing the current computational results with the information supplied was done as the second validation phase. [20] As illustrated in Table 4. The theoretical model presented by [20] was developed considering a thermoelectric unit with one symmetrical pair of semiconductors with a length and width of 1 mm, and height of 0.8 mm. It should be mentioned that, as the melting point of the solder material is around 485 °C, the operating temperature of the thermometric units is kept between 50 °C and 150 °C for T_h. while, T_c is kept constant at 20 °C. The semiconductors, conducting plates, and adhesive layers were built of Bi_2Te_3, Cu and Sn–Pb, accordingly and internal resistance of the semiconductors

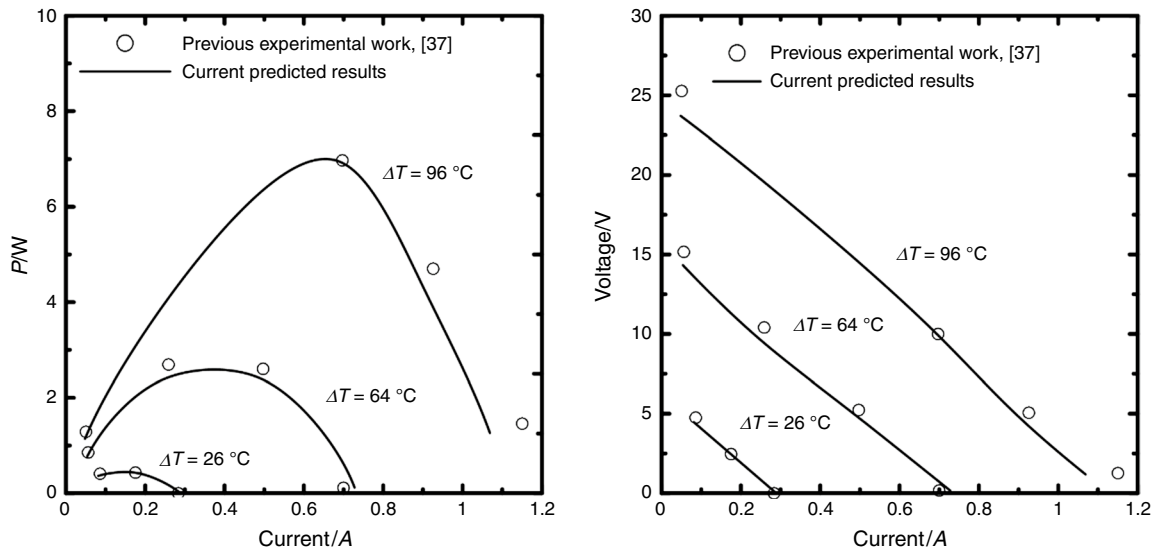

Fig. 6 A comparison of the findings of the present work with those mentioned in [37]

Table 4 Validation results with Ma et al. [20]

Parameter	Current model			Ma et al. [20]			Error/%		
ΔT	30 °C	80 °C	130 °C	30 °C	80 °C	130 °C	30 °C	80 °C	130 °C
P	0.00146	0.01037	0.029	0.00140	0.01	0.03	4.02	3.50	3.45
η	0.921	2.45682	3.99	0.920	2.39	3.80	0.14	2.72	4.82

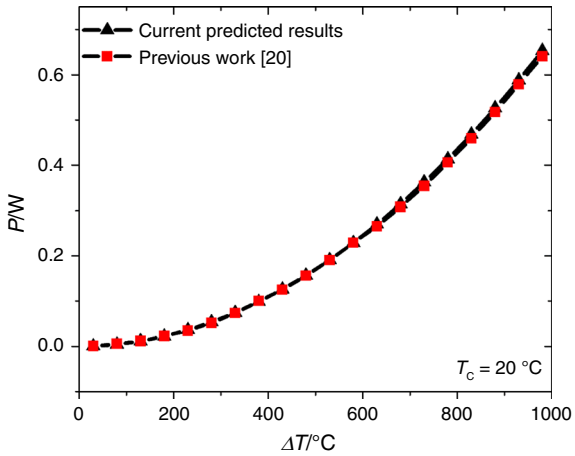

Fig. 7 A comparison between the predicted findings of power output and those provided in [20]

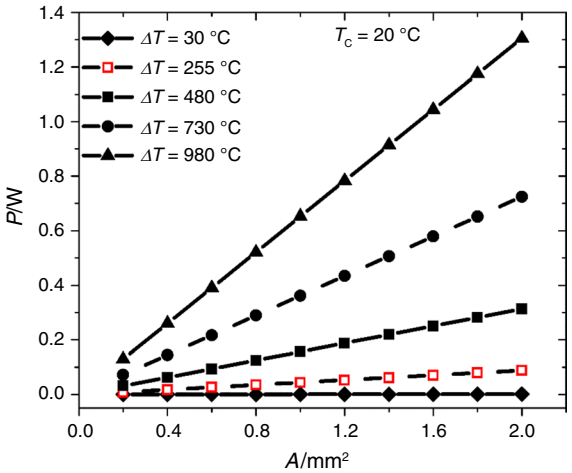

Fig. 8 Effects of leg cross-sectional area on the output power at difference values of temperature difference

was roughly 3.12×10^{-2} Ω. Ma et al. [20] numerically predicted the maximum power output along with the maximum efficiency at varying T_h from 50 °C to 150 °C, and $T_2 = 20$ °C. The current predicted results agree with data of the numerical maximum power output along with the maximum efficiency in [20] with maximum error of around 4%, 4.8% as shown in Table 4 in the maximum power output and maximum efficiency, respectively.

The computational model presented by [20] used a thermoelectric unit without solder layers to study the effect of the higher T_h on the system performance. The theoretical model used by [20] was a thermoelectric unit with one symmetrical pair of semiconductors with a length of 1.00 mm, width of 1.00 mm and height equals to 0.96 mm. In furthermore, there are three conducting plates: two in the bottom with dimensions of 1.40 mm1.00 mm and one in the top with dimensions of 2.80 mm1.0 mm for length and width, respectively. Each of them has a height of 0.25mm.The semiconductors material was SiGe with internal resistance of around 1.92×10^{-2} Ω. Ma et al. [20] numerically predicted the maximum power output at changing the T_h from 50 °C to 1000 °C, at $T_2 = 20$ °C. Figure 7 displays the electrical power output results along with the associated numerical values. The present predicted findings and the numerical results of [20] are consistent, as shown in figure, with the largest relative error of 0.8%.

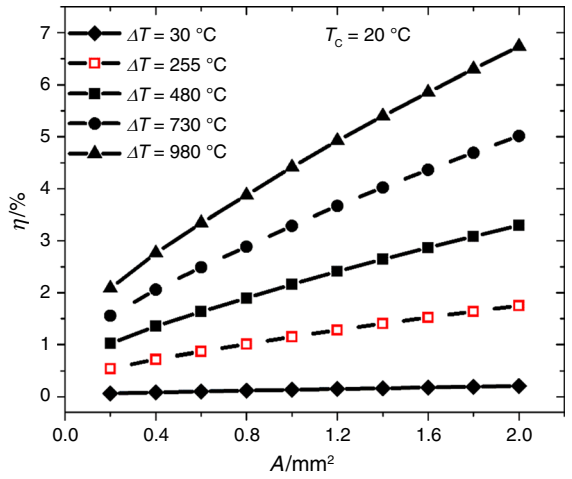

Fig. 9 Effects of leg cross-sectional area on the efficiency of *P–N* legs at difference values of temperature difference

The effect of the design variables on the TEG performance

The design variables include the leg length, cross section and strip thickness. Figures 8 and 9 show the effects of leg cross-sectional area on the power output and efficiency,

respectively, at constant leg length L equals 0.96 mm and strip thickness t_p of 0.25 mm.

Figure 8 presents the predicted values of output power at different values of temperature difference (30°C, 480 °C and 980°C) and leg cross-sectional area ranged from 0.2 to 2.0 mm^2. At specific temperature difference, the output power increases linearly with cross-sectional area. This is reported by Ma [20] as they concluded that at a constant leg length, power is enhanced by leg cross-sectional area increase. When the area increases from 0.2 mm^2 to 2.0 mm.^{2}, the output power increases by about 2%, 200% and 1200% at 30°C, 480°C and 980°C, respectively. The explanation of power increase under TEG leg cross-sectional area enlargement is due to the reduction happened in the internal resistance of TEG material and increase in its mass which enhances the Seebeck effect over the Peltier effect. As a result, more electricity energy rate is generated over thermal energy rate. Seebeck effect is the amount of electricity could be extracted from the heat transferring through TEG material. Nevertheless, Peltier effect shows the reverse process of the conversion of electricity into thermal energy inside the material of TEG as explained in [1]

The output power at a specific cross-section area, such 2.0 mm^2, is proportional to the magnitude of temperature differential. When the temperature difference increases from 30 °C to 980 °C, the output power increases from 0.03 W to its maximum value 1.3 W. Generally, increasing the cross section or temperature difference allows more heat to pass through the material of TEG which means more power generated. It is noticed that the power generation starts above 50 °C temperature difference.

Figure 9 presents the predicted values of efficiency at different values of temperature difference (30 °C, 480 °C and 980 °C) and leg cross-sectional area ranged from 0.2 to 2 mm^2. At specific temperature difference, the efficiency increases linearly with cross-sectional area increase. When the area increases from 0.2 mm^2 to 2mm^2, the efficiency increases by about 0%, 250% and 250% at 30 °C, 480 °C and 980 °C,, respectively. At a certain cross-section area such as 2.0 mm^2, the efficiency is proportionally increases with the value of temperature difference. When the temperature difference increases from at 30 °C to 980 °C the efficiency increases from 0% to its maximum value 6.7%. The increasing of the cross section or temperature difference allow more heat to pass through the material of TEG which means more rate of heat conversion into electricity. The maximum reached conversion efficiency is about 6.7% at 980 °C temperature difference between hot and cold TEG sides.

Figure 10 presents the predicted values of output power at different values of temperature difference (30 °C, 480 °C and 980 °C) and leg length ranged from 0.5 to 4 mm at constant leg cross-sectional area A equals 1 mm^2 and t_p of 0.25 mm. At specific temperature difference, the output power decreases dramatically with the increase in leg length. When the length increases from 0.5 to 4 mm (700% increase rate), the output power decreases by about 0%, 200% and 500% at 30 °C, 480 °C and 980 °C, respectively. For more details, the effect of TEG leg length on power generated can be explained. the increase TEG leg length causes an increase in the internal resistance of TEG which consequently enhances the Peltier effect over the Seebeck effect and that means more thermal energy rate generation from electricity over electric energy rate generation from input heat.

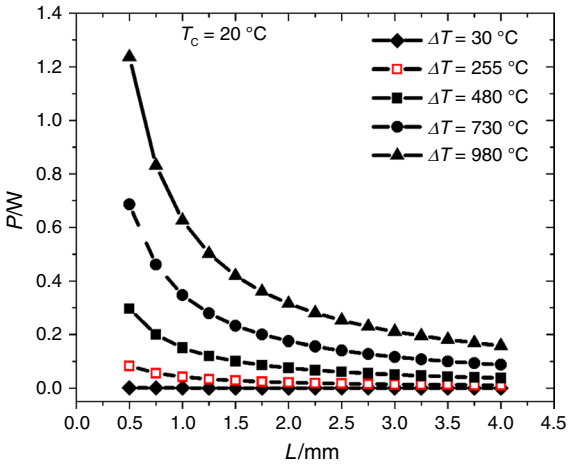

Fig. 10 Effects of leg length on the output power of *P–N* legs at difference values of temperature difference

On the other hand, at constant leg length, the output power generation is strongly depending on the temperature difference. At specific leg length such as 0.5 mm where the temperature difference increases from 30 °C to 980 °C, the output power increases from 0.03 to1.3 W.

Figure 11 presents the predicted values of efficiency at different values of temperature difference (30 °C, 480 °C and 980 °C), and leg length ranged from 0.5 to 4 mm. At specific temperature difference, the efficiency decreases dramatically with the increase in leg length. When the length increases from 0.5 to 4 mm, efficiency decreases by about 3%, 14% and 16% at 30 °C, 480 °C and 980 °C,, respectively.

On the other hand, at constant leg length, the conversion efficiency is strongly depending on the temperature difference. At specific leg length such as 0.5 mm when temperature difference increases from 30 °C to 980 °C, the output power increases from 0 to 4.5%. The maximum value of efficiency at 1 mm^2 cross-sectional area and t_p of 0.25 mm was about 4.5% at leg length of 0.5 mm, and 980°C. The reason of power reduction when TEG leg length increase is that the increase in TEG leg length causes an increase in the internal resistance of TEG which subsequently enhances the

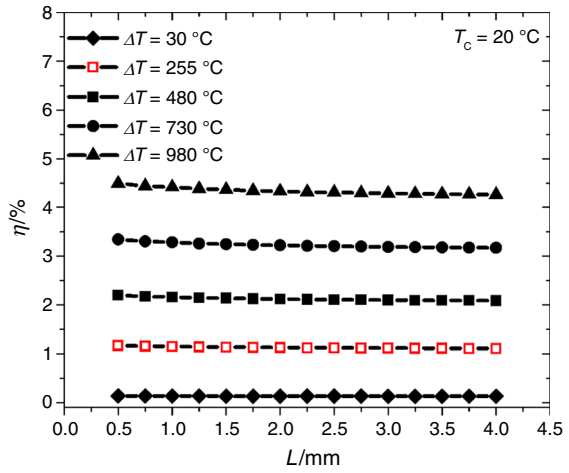

Fig. 11 Effects of leg length on the efficiency of *P–N* legs at difference values of temperature difference

Peltier effect over the Seebeck effect and that means more thermal energy rate generation over electric energy rate generation. Seebeck effect is the amount of electricity could be extracted from the heat transferring through TEG material. Nevertheless, Peltier effect shows the reverse process of the conversion of electricity into thermal energy inside the material of TEG as explained in [1].

Figure 12 presents the predicted values of output power at different values of temperature difference (30 °C, 480 °C and 980 °C), strips thickness ranged from 0.1 to 1 mm at constant leg length L equals 0.96 mm and cross-sectional area A of 1 mm^2. At all temperature difference, the change of strip thickness has a negligible effect on the value of the output power. At specific thickness, the increase in temperature difference from 30 °C, to 980 °C causes an increase in output power from 0.01 W to 0.65 W, respectively. On the other hand, at constant strips thickness, output power is strongly depending on the temperature difference. At specific strips thickness such as 0.1 mm when temperature difference increases from 30 °C to 980 °C, the output power increases from 0 to 0.65W.

Figure 13 presents the predicted values of efficiency at different values of temperature difference (30 °C, 480 °C and 980 °C), and strips thickness ranged from 0.1 to 1 mm.

At all temperature difference, the change of strip thickness has negligible effect on the value of the conversion efficiency. According to Fourier's law of heat condition, at constant temperature difference and cross-sectional area, the higher strip thickness reduce slightly the transferred thermal energy relative to the generated electricity between TEG hot and cold side and consequently enhance its conversion efficiency. But with very small value as the change of strip thickness is very small compared with leg length.

Nevertheless, at specific thickness, the increase in temperature difference from 30 °C, to 980 °C causes an increase in efficiency from 0.1% to 4.5%, respectively.

Comparison between the performance parameter of the modified and conventional thermoelectric unit

As mentioned before, the theoretically current study was performed through two main steps. First, to estimate the effects of each design variable (parameter) on the output power and efficiency of *P–N* couple as seen in Section "Model validation". Then, the optimization technique is used to find the best design for the TEG system as detailed in the previous subsection (5.2). The chosen *P–N* couple's performance is next investigated numerically using the best design variables

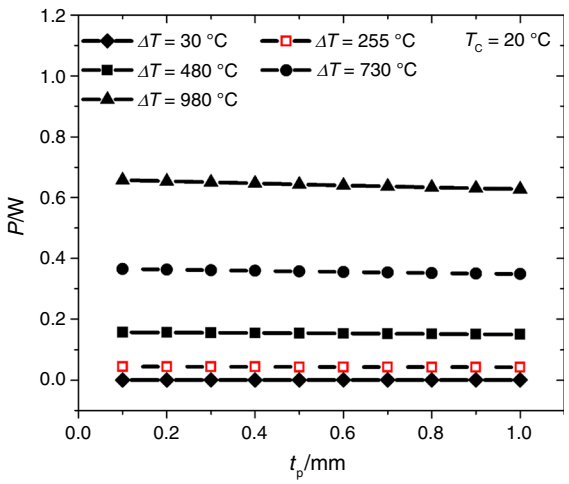

Fig. 12 Effects of strip thickness on the output power of *P–N* legs at difference values of temperature difference

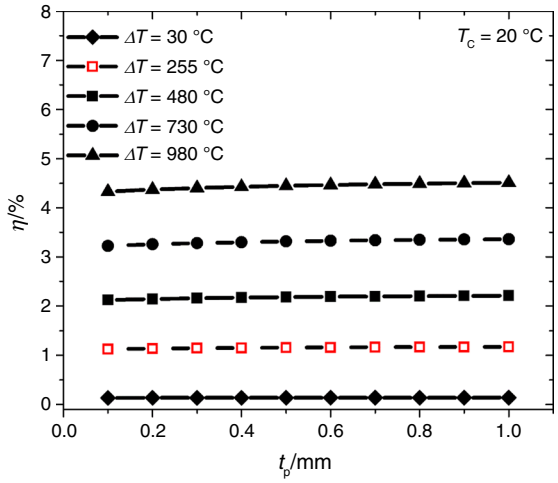

Fig. 13 Effects of strip thickness on the efficiency of *P–N* legs at difference values of temperature difference

that were previously picked from Section "The effect of the design variables on the TEG performance". Then, the results will be compared to the conventional system presented by [20].

Figure 14 presents the predicted values of output power of the optimized *P–N* couple compared with that of the conventional system introduced by [20]. The applied temperature difference ranges from 30°C to 980 °C. As shown, the increasing the temperature difference enhances the output power generated from both systems. However, the increasing rate of power generated from the modified and optimized system is higher than conventional system [20]. These rate jumps dramatically from 1 to 273% when temperature difference varies from 30 °C to 980 °C, respectively. The maximum generated power at 980 °C about 2.39 W and 0.64 W for modified system and conventional system, respectively. Finally, the enhancement in TEG generated power due to the proposed design is about 273% over the conventional system. This enhancement is due to the higher effect of Seebeck over the effect of Peltier effect as explained in the previous lines.

Figure 15 presents the predicted values of conversion efficiency of the optimized *P–N* couple comparing with the conventional system. As shown, the increasing of temperature difference enhances the conversion efficiency from both the proposed modified and conventional systems. However, the increasing rate of conversion efficiency from the modified and optimized system is higher than that of conventional system. Moreover, these rates increase moderately from 1 to 12% when temperature difference jumps from 30 °C to 980 °C, respectively. The maximum generated power at 980 °C about 5.73% and 4.9% for modified system and conventional system, respectively.

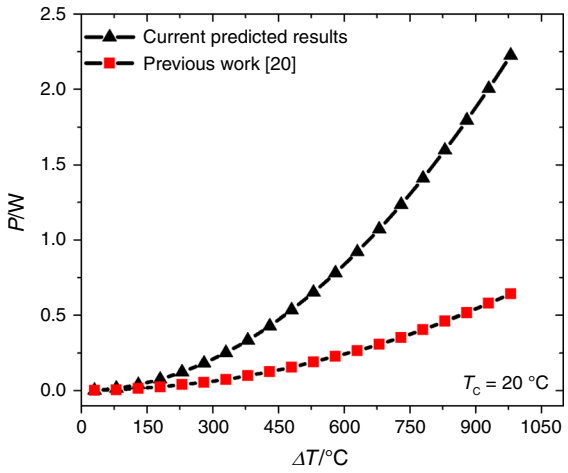

Fig. 14 Comparison between the power output of the modified and conventional thermoelectric unit at different ΔT, $T_c = 20$ °C

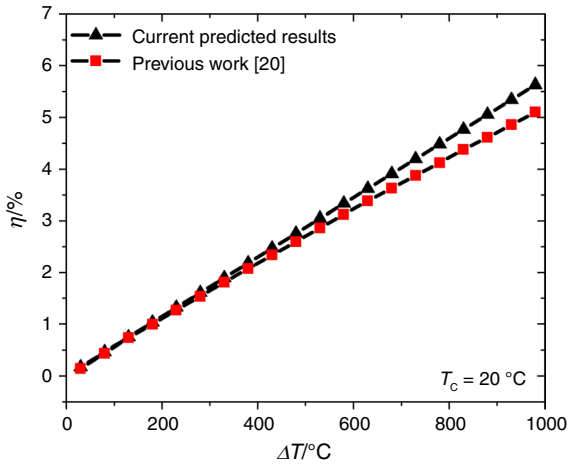

Fig. 15 Comparison between the current predicted conversion efficiency and that obtained by conventional TEG proposed by [20]

Figure 16 summarizes the overall change in the power and conventional efficiency for both proposed modified optimized and the conventional system. This figure illustrates clearly the enhanced happened in the TEG generated power and conventional efficiency due the proposed design presented by the author. As shown, the maximum achieved enhancement in TEG generated power due to the proposed design is about 273% over the conventional system. Moreover, the maximum increasing rate of conversion efficiency due to the proposed design is about 12% over the conventional system at 980 °C temperature difference between hot and cold side.

Figure 16 summarizes all studied cases. As shown, the updated and optimized system over the traditional system is clearly defined with a comprehensive growing rate for output power and conversion efficiency as a function of temperature

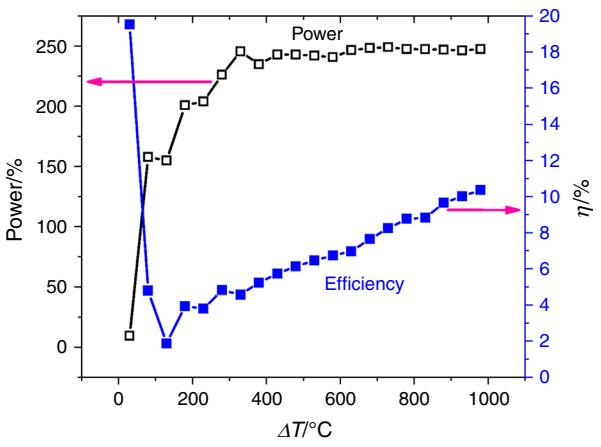

Fig. 16 Variation of the power output and the conversion efficiency compared with the conventional TEG of [20]

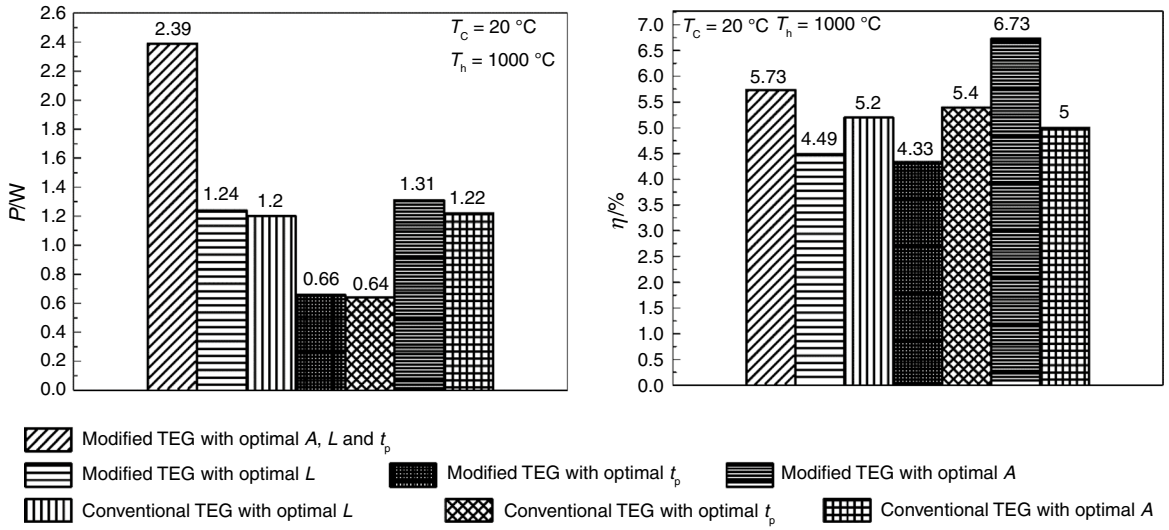

Fig. 17 Comparison between the modified and conventional TEG proposed by [20] at temperature difference of 980 °C

difference. a comparison between the maximum performance parameters can be achieved by the optimal TEG obtained by based surrogate model with that obtained by predicted optimal variables that detailed in Section "Model validation" (A, L and t_p) and with that reported by [20] at temperature difference of 980 °C. The fundamental TEG sizes for A and t_p are 1.0 mm2, 0.96 mm, and 0.25 mm, accordingly (Fig. 17).

As presented in this figure, the modified TEG achieves a significant enhancement in the generated power and the conversion efficiency compared with that obtained by both single variable effect and that reported by [20]. For instance, at the same temperature difference of 980 °C, the maximum output power of the modified TEG, predicated TEG with optimal L, predicated TEG with optimal t_p, predicated TEG with optimal A, conventional TEG with optimal L [20], conventional TEG with optimal t_p [20] and conventional TEG with optimal A [20] are 2.39, 1.24, 0.66, 1.31,1.2,0.64 and 1.22, respectively. While for the conversion efficiency, the predicated TEG with optimal A provide the higher value of 6.7% compared with 5.73% that obtained by the modified TEG with optimal A, L, and t_p. This is reduction in the efficiency due to the steady state heat input in the case of the modified TEG with optimal A, L and t_p is higher than that achieved in the predicted TEG with optimal A (Fig. 17).

Conclusion

It is suggested to redesign a TEG system. Along with altering the copper strip thickness, it also varies the leg length and cross-sectional area. An extensive three-dimensional model of the thermoelectric generator is created to assess the impact of the innovative design on the TEG performance. Since the key discoveries, the following can be drawn. It is found that changing the leg cross-sectional area and the leg length have a substantial impact on the TEG performance by examining the effects of each design component separately. While the TEG performance is unaffected by the strip thickness at all temperature ranges. The optimization technique is used to consider the interactions between all design variables. By examining the optimal design, it is found that the predicted TEG from the surrogate-based optimization can generate higher output power compared with both achieved by the single variables effect and the conventional one. The findings of current study enable researchers to achieve more output power and conversion efficiency by utilizing the optimal TEG.

Funding Open access funding provided by The Science, Technology & Innovation Funding Authority (STDF) in cooperation with The Egyptian Knowledge Bank (EKB).

References

1. Radhakrishnan R. A Review of: "Thermoelectric Handbook, Macro to Nano, D.M. Rowe (editor)." Mater Manuf Process. 2008; 23:626–7. https://doi.org/10.1080/10426910802135819
2. Chen W-H, Wu P-H, Lin Y-L. Performance optimization of thermoelectric generators designed by multi-objective genetic algorithm. Appl Energy. 2018;209:211–23.
3. Champier D, Bédécarrats JP, Kousksou T, Rivaletto M, Strub F, Pignolet P. Study of a TE (thermoelectric) generator incorporated in a multifunction wood stove. Energy. 2011;36:1518–26.
4. Niu X, Yu J, Wang S. Experimental study on low-temperature waste heat thermoelectric generator. J Power Sources. 2009;188:621–6.
5. Francioso L, De Pascali C, Siciliano P. Experimental assessment of thermoelectric generator package properties: simulated results validation and real gradient capabilities. Energy. 2015;86:300–10.
6. Yazawa K, Hao M, Wu B, Silaen AK, Zhou CQ, Fisher TS, et al. Thermoelectric topping cycles for power plants to eliminate cooling water consumption. Energy Convers Manag. 2014;84:244–52.
7. Meng F, Sun F. Effects of temperature dependence of thermoelectric properties on the power and efficiency of a multielement thermoelectric generator. Int J Energy Environ. 2012;3(1):137–50.
8. Abdo A, Ookawara S, Ahmed M. Performance evaluation of a new design of concentrator photovoltaic and solar thermoelectric generator hybrid system. Energy Convers Manag. 2019;195:1382–401. https://doi.org/10.1016/j.enconman.2019.04.093.
9. Kanimba E, Tian Z. A new dimensionless number for thermoelectric generator performance. Appl Therm Eng. 2019;152:858–64.
10. Wang H, Li J, Zou M, Sui T. Synthesis and transport property of AgSbTe2 as a promising thermoelectric compound. Appl Phys Lett. 2008;93:202106.
11. Pei Y, Lalonde A, Iwanaga S, Snyder G. High thermoelectric figure of merit in heavy hole dominated PbTe. Energy Environ Sci. 2011;4:2085.
12. Dow H, Oh M, Kim B, Park S, Min B, Lee HW, et al. Effect of Ag or Sb addition on the thermoelectric properties of PbTe. J Appl Phys. 2010;108:113709.
13. Levin E, Hanus R, Hanson M, Straszheim W, Schmidt-Rohr K. Thermoelectric properties of Ag2Sb2Ge 46 - XDyxTe50 alloys with high power factor. Phys status solidi. 2013;210:2628.
14. Ivanova LD, Granatkina YV. Thermoelectric properties of Bi2Te3-SB2Te3 single crystals in the range 100–700 K. Inorg Mater. 2000;36:672–7.
15. Zare V, Palideh V. Employing thermoelectric generator for power generation enhancement in a Kalina cycle driven by low-grade geothermal energy. Appl Therm Eng. 2018;130:418–28.
16. Shu G, Zhao J, Tian H, Liang X, Wei H. Parametric and exergetic analysis of waste heat recovery system based on thermoelectric generator and organic rankine cycle utilizing R123. Energy. 2012;45:806–16.
17. Daghigh R, Khaledian Y. A novel photovoltaic/thermoelectric collector combined with a dual – Evaporator vapor compression system. Energy Convers Manag. 2018;158:156–67.
18. Akhlaghi Garmejani H, Hossainpour S. Single and multi-objective optimization of a TEG system for optimum power, cost and second law efficiency using genetic algorithm. Energy Convers Manag. 2021;228:113658. https://doi.org/10.1016/j.enconman.2020.113658.
19. Sunderland JE, Burak NT. The influence of the Thomson effect on the performance of a thermoelectric power generator. Solid State Electron. 1964;7:465–71.
20. Ma Q, Fang H, Zhang M. Theoretical analysis and design optimization of thermoelectric generator. Appl Therm Eng. 2017;127:758–64. https://doi.org/10.1016/j.applthermaleng.2017.08.056.
21. Shen ZG, Wu SY, Xiao L, Yin G. Theoretical modeling of thermoelectric generator with particular emphasis on the effect of side surface heat transfer. Energy. 2016;95:367–79. https://doi.org/10.1016/j.energy.2015.12.005.
22. Oh MW, Ahn JH, Lee JK, Kim BS, Park SD, Min BK, et al. Estimation of power generation from thermoelectric devices: model analysis and performance measurements. Electron Mater Lett. 2010;6:129–34.
23. Ali H, Sahin AZ, Yilbas BS. Thermodynamic analysis of a thermoelectric power generator in relation to geometric configuration device pins. Energy Convers Manag. 2014;78:634–40.
24. Yamashita O. Effect of linear and non-linear components in the temperature dependences of thermoelectric properties on the cooling performance. Appl Energy. 2009;86:1746–56.
25. Wang Y, Dai C, Wang S. Theoretical analysis of a thermoelectric generator using exhaust gas of vehicles as heat source. Appl Energy. 2013;112:1171–80.
26. Ali H, Yilbas BS. Influence of pin material configurations on thermoelectric generator performance. Energy Convers Manag. 2016;129:157–67.
27. Kalteh M, Akhlaghi GH. Investigating the influence of Thomson effect on the performance of a thermoelectric generator in a waste heat recovery system. Int J Green Energy. 2019;16:917–29. https://doi.org/10.1080/15435075.2019.1642896.
28. Zhang F, Cheng L, Wu M, Xu X, Wang P, Liu Z. Performance analysis of two-stage thermoelectric generator model based on Latin hypercube sampling. Energy Convers Manag. 2020;221:113159.
29. Liu J, Zhang Y, Zhang D, Jiao S, Zhang Z, Zhou Z. Model development and performance evaluation of thermoelectric generator with radiative cooling heat sink. Energy Convers Manag. 2020;216:112923.
30. Arora R, Arora R. Multicriteria optimization based comprehensive comparative analyses of single- and two-stage (series/parallel) thermoelectric generators including the influence of Thomson effect. J Renew Sustain Energy. 2018;10:44701. https://doi.org/10.1063/1.5019972.
31. Marvão A, Coelho PJ, Rodrigues HC. Optimization of a thermoelectric generator for heavy-duty vehicles. Energy Convers Manag. 2019;179:178–91. https://doi.org/10.1016/j.enconman.2018.10.045.
32. Dongxu J, Zhongbao W, Pou J, Mazzoni S, Rajoo S, Romagnoli A. Geometry optimization of thermoelectric modules: Simulation and experimental study. Energy Convers Manag. 2019;195:236–43.
33. Sun H, Ge Y, Liu W, Liu Z. Geometric optimization of two-stage thermoelectric generator using genetic algorithms and thermodynamic analysis. Energy. 2019;171:37–48.
34. Nozariasbmarz A, Suarez F, Dycus JH, Cabral MJ, LeBeau JM, Öztürk MC, et al. Thermoelectric generators for wearable body heat harvesting: Material and device concurrent optimization. Nano Energy. 2020;67:104265.
35. Jaziri N, Boughamoura A, Müller J, Mezghani B, Tounsi F, Ismail M. A comprehensive review of thermoelectric generators: technologies and common applications. Energy Reports. 2020;6:264–87.
36. Statistics and Machine Learning Toolbox - MATLAB, (2022). https://www.mathworks.com/products/statistics.html (accessed August 20, 2022).
37. Yang W, Xie H, Sun L, Ju C, Li B, Li C, et al. An experimental investigation on the performance of TEGs with a compact heat exchanger design towards low-grade thermal energy recovery. Appl Therm Eng. 2021;194:117119.